Fuse Sizing Using Penetration Level Indicators in IBR-dominated Distribution Feeders

Murillo Cobe Vargas, Oureste Elias Batista, and Yongheng Yang

***Abstract*—This paper proposes a methodology for sizing fuse links in distribution feeders to accommodate large-scale inverter-based resources (IBRs), employing an indicator for the maximum allowable penetration level of IBRs on a lateral branch. The impact of high IBR penetration on fuse link operation during various faults is analyzed. Simulations are performed in MATLAB/Simulink using the IEEE 34-Node Test Feeder as a case study. The results demonstrate the methodology's effectiveness in ensuring the protection of lateral branch conductors while preventing unintended tripping due to faults outside the protection zone. Analyses of penetration levels for existing fuses and fuse replacements are presented and discussed. The findings confirm that resizing fuses can enable higher IBR integration without requiring additional infrastructure, making use of existing equipment while maintaining overcurrent protection coordination.**

***Keywords*—Communication-free, distribution feeders, fuses, inverter-based resources, overcurrent protection.**

I. Introduction

ELECTRIC power systems are facing challenges with the rapid installation of distributed energy resources (DERs) [1]. In this context, electronically-coupled or inverter-based resources (IBRs) are rapidly increasing in both power capacity and quantity. Consequently, the short-circuit current (SCC) level of a distribution feeder can change significantly, despite the small power capacities from IBRs, affecting traditional protection schemes in distribution systems [2], [3], [4]. Therefore, the fuses that protect distribution feeder lateral branches may trip incorrectly–either failing to meet fuse-saving philosophies, blowing unnecessarily, or allowing the conductor to carry a higher current than its limit.

Most studies related to fuse protection in electrical networks with the high penetration of IBRs focus on modifying the performance characteristics of reclosers to maintain the fuse-saving scheme [5], since fuse parameters cannot be modified (i.e., adapted) but only replaced with another one. For instance, in the work of Dugan and Rizy (1984) [6], the effect of fault types and the penetration level of distributed generators on fuse melting time is investigated. A fuse-sizing method is proposed to maintain coordination, but it does not cover all short circuits types, and it considers distributed generators as induction generators. Based on the authors' extensive literature review, no other work was found that addresses fuse sizing in the context of distributed generation.

To maintain the fuse-saving scheme, the following options are available: 1) disconnecting the IBR; 2) limiting the penetration level; 3) using fault current limiters (FCLs); 4) implementing adaptive protection. Regarding option 1), it is the simplest way to maintain the fuse-saving scheme. However, it is an inefficient approach seen from a technical point of view, since faults are predominantly transient events, and there are also the effects of generator resynchronization [7], [8]. Option 2) is also a simple strategy, but it can limit the benefits of implementing DERs in distribution networks [9], [10]. For option 3), the use of FCLs requires a high initial investment, and detailed analyses are necessary to choose the best type, best location, and the appropriate resistance for implementation [11], [12], [13], [14], [15]. Option 4) modifies the parameters of the overcurrent protection devices (OCPDs) curves, but it may require communication links, making its implementation costly. Certain works do not use communication links [16], [17], [18], but they do not consider fuse sizing. The work of Barranco-Carlos *et al.* (2023) [19] provides an extensive literature review on adaptive protection in networks with DERs. Fuses are rarely considered, nor is the optimal adjustment of their operating curves [20]. Finally, considering a different approach from the previous ones, the work of Agarwal *et al.* (2023) [21] presents a fuse prototype (iFuse) for networks with the high integration of IBRs. The prototype uses a power electronics circuit, which performs monitoring and control, integrated into a traditional fuse.

In light of the above, this paper presents a methodology for sizing the fuse link of a distribution feeder with the presence of IBRs to avoid unintended tripping and to protect the lateral branch conductor by introducing a penetration level indicator. The methodology does not require communication links or equipment with characteristics different from those already in use. The effectiveness of the approach is demonstrated using the IEEE 34-Node Test Feeder with MATLAB/Simulink simulations.

II. Fuse Sizing and IBRs Integration Impacts

The fuses of a distribution feeder generally protect lateral branches and can be sized by [22], [23]

$$1.5I_{load-max} \simeq I_{fuse} \leq \frac{1}{4}I_{ph-min} \tag{1}$$

This study was supported in part by the Coordenacao de Aperfeicoamento de Pessoal de Nivel Superior - Brazil (CAPES) - Finance Code 001.

M. C. Vargas is with the Federal Institute of Espirito Santo, Guarapari, 29216-795 Brazil (e-mail: murillo.vargas@ifes.edu.br; mvargas@ieee.org).

O. E. Batista is with the Federal University of Espirito Santo, Vitoria, 29075-910 Brazil (e-mail: oureste.batista@ufes.br).

Y. Yang is with the College of Electrical Engineering, Zhejiang University, Hangzhou, 310027 China (e-mail: yoy@zju.edu.cn)

Paper submitted to the International Conference on Power Systems Transients (IPST2025) in Guadalajara, Mexico, June 8-12, 2025.

where I_{fuse} is the rated fuse current, $I_{load-max}$ is the load current of the protected lateral branch at a heavy load level, and I_{ph-min} is the fault current for a bolted line-to-ground (LG) fault at the end of the lateral branch. In (1), the fraction value of I_{ph-min} can be $\frac{1}{4}$ up to $\frac{3}{4}$ of the bolted LG fault or 100% of the LG fault with a fault resistance (it may vary from utility to utility), both considered at the end of the lateral branch or protected zone [22].

In a scenario with a high penetration level of IBRs installed on a lateral branch, four different situations may affect the fuse operation, as represented in Fig. 1.

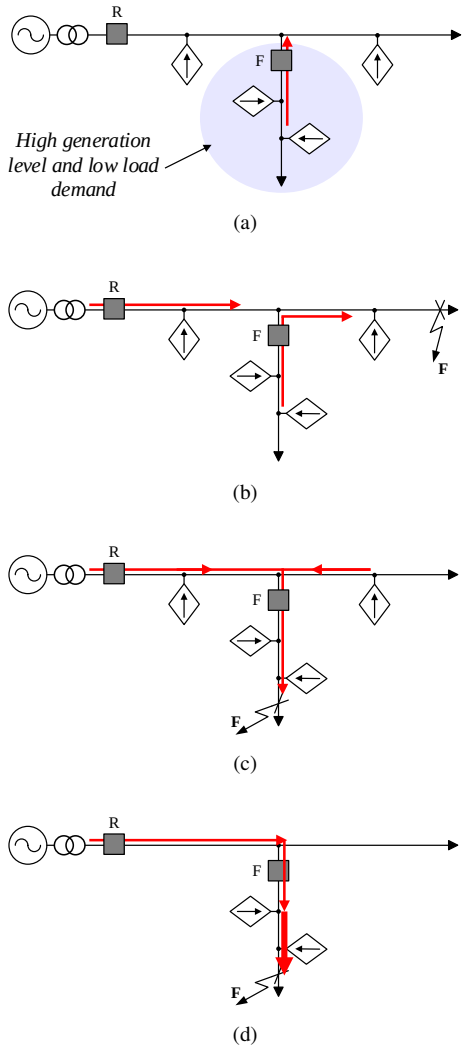

Fig. 1: Effect of the high IBR penetration levels on fuse protection. (a) Tripping of fuse (F) due to low load demand on the lateral branch and high generation level. (b) Unintended tripping of fuse (F) caused by a fault on the main feeder trunk. (c) Impact on fuse-blow or fuse-save schemes during a lateral branch fault. (d) Different short-circuit current levels through the lateral branch conductor.

A. Fuse Tripping Under Feeder's Normal Operation Condition

For a feeder under normal operation with low load demand on the lateral branch and a high generation level from the IBRs, as presented in Fig. 1(a), the current from IBRs will supply the nearest loads and the net power will supply the loads on the main trunk, making the current flow in reverse through the fuse. If the current through the fuse (I_{FS}) is greater than I_{fuse}, it may trip, disconnecting the lateral branch. The worst scenario for this situation is when there is maximum generation from IBRs and a zero or very low load demand from the lateral branch.

Hence, the previous value of $1.5I_{load-max}$ used in (1) to calculate I_{fuse} can be lower than the actual current through the conductor due to the presence of IBRs. In Brazilian regulations, for example, the DER rated power for small consumer units (residential, commercial, and small industries) is limited to the "breaker rated power", i.e., phase-to-neutral voltage times the breaker's nominal current per phase, which is generally higher than the maximum demand of the consumer unit. Scaling this up to other consumer units, the previously explained situation can occur. In this case, it may be assumed that (1) is disrupted if

$$\sum_{i=1}^{n} I_{i-ibr} \geq I_{fuse} \text{ or } \sum_{i=1}^{n} I_{i-ibr} \geq 1.5I_{load-max} \quad (2)$$

where $\sum_{i=1}^{n} I_{i-ibr}$ is the sum of the nominal currents of n IBRs installed on the protected lateral branch. If one of the conditions above is reached, the appropriateness of the fuse sizing must be evaluated.

B. Fuse Tripping for a Fault Outside Lateral Branch

Assuming a fault condition on the main trunk, as shown in Fig. 1(b), the IBRs installed on the lateral branch, downstream from the fuse, may contribute with SCCs to the fault point. In this case, an unintended disconnection of the lateral branch may occur due to the fuse tripping for a fault outside its protection zone. Assuming an SCC contribution from IBRs (SCC) in p.u., the total current contribution of IBRs in this condition can be $SCC \cdot \sum_{i=1}^{n} I_{i-ibr}$. Each IBR installed may contribute to the fault point with different SCC. It can be considered the rule of thumb value of $SCC = 1.2$ p.u., maximum fault current contribution, for this case, although it may vary from different factors.

The fault current characteristics of legacy inverters during faults differ significantly from those of inverters that comply with modern grid codes. Legacy inverters are quickly disconnected from the grid, whereas modern ones are required to exchange power during faults providing grid support, following the grid code curves. The pre-fault operating conditions of IBRs–such as active and reactive power exchange with the grid–determined by modern grid codes (e.g., IEEE Std 1547-2018 [24]), along with voltage variations at the point of connection (PoC), influence internal current control loops. As a result, IBRs may operate with different phase angles, reducing their total fault current contribution. IBRs located closer to the fault point may experience severe voltage sags at the PoC, potentially leading to a complete cessation of fault current injection and further decreasing the total fault current contributions. Conversely, IBRs positioned farther from the fault point along the upstream feeder may experience smaller voltage variations at the PoC, preventing

them from reaching the condition for maximum fault current injection.

Considering that the current through the fuse in a fault condition is $SCC \cdot \sum_{i=1}^{n} I_{i-ibr}$, Eq. (1) is disrupted if

$$SCC \cdot \sum_{i=1}^{n} I_{i-ibr} \geq I_{fuse} \text{ or } SCC \cdot \sum_{i=1}^{n} I_{i-ibr} \geq 1.5 I_{load-max} \tag{3}$$

If one of the conditions above is reached, the fuse sizing must be evaluated.

C. Fuse Tripping for a Fault on the Lateral Branch

For a fault on the lateral branch, as shown in Fig. 1(c), the fuse F must operate according to the protection scheme proposed: fuse-blow or fuse-save. For the fuse-save scheme, the fault current contribution from IBRs located on the main trunk, upstream from F, will increase the current through it and decrease the current through R. It may lead to a faster operation of F compared to R, potentially disrupting the fuse-save scheme, making F trip before R and disconnecting the lateral branch. For the fuse-blow scheme, the fault current contribution from IBRs located on the lateral branch will decrease the current through F and R. As discussed in [25], the current decrease will be more severe for F than R if more IBRs are installed on the lateral branch than on the main trunk, which may disrupt the fuse-blow scheme. Most papers discuss modifying the settings of relays/reclosers upstream of the fuses to overcome these issues.

D. Conductor Above its Conduction Limit

For a fault on a lateral branch with the integration of IBRs downstream of the fuse, as shown in Fig. 1(d), the conductor of the lateral branch may experience different SCC values depending on the point of installation of IBRs, as indicated by the thickness of the arrows. Depending on the penetration level of IBRs on the lateral branch, the SCC contribution of IBRs downstream of the fuse will increase the current through the conductor compared to points closer to it. This higher current value flowing through the conductor may exceed its conduction limit and cause deterioration.

III. Proposal for Fuse Sizing

The maximum current that can flow backward through a fuse in the presence of IBRs installed downstream is given by $SCC \cdot \sum_{i=1}^{n} I_{i-ibr}$, as discussed in the above. Consequently, the bolted LG fault current at the end of the fuse protection zone may be lower than that in a scenario without IBRs. In light of the above, Eq. (1) can be modified to consider these new boundary conditions:

$$max\{1.5 I_{load-max}; SCC \cdot \sum_{i=1}^{n} I_{i-ibr}\} \leq I_{fuse} \leq \frac{1}{4} I_{ph-ibr} \tag{4}$$

in which I_{ph-ibr} is the bolted LG fault current at the end of the fuse protection zone with IBRs.

To explore the applications and validate the proposed scheme, approaches to protect the conductor from overcurrents above its limits and avoid the unintended tripping of the fuse will be explored in the following sections.

A. Avoiding Unintended Tripping

Unintended tripping of the fuse can occur when, in reverse, the current through the fuse is greater than its minimum melting current, leading to incorrect tripping. The fuses that will be used as references in this work are the S&C Electric Company "K" Speed Positrol Fuse Links [26]. In most cases, the minimum current to initiate the link melting is at least twice its nominal value.

Considering F_{melt} as the multiple of the fuse rated current that causes it to start melting, the unintended tripping may occur or be imminent when the reverse current through the fuse is at least F_{melt} times the rated current of the fuse. For S&C Electric Company "K" Speed Positrol Fuse Links, $F_{melt} \approx 2$. Hence, the maximum current that IBRs can inject in reverse through the fuse without tripping it can be given by

$$SCC \cdot \sum_{i=1}^{n} I_{i-ibr} \leq F_{melt} \cdot I_{fuse} \tag{5}$$

Applying Eq. (5), it is possible to calculate an IBR penetration level (PL), in relation to the heavy load current on the lateral branch, which may avoid unintended tripping of the fuse. Rearranging Eq. (5), gives

$$\sum_{i=1}^{n} I_{ibri} \leq \frac{F_{melt} \cdot I_{fuse}}{SCC} \tag{6}$$

Since the IBRs and the loads connected to the lateral branch are at the same voltage level, the PL of IBRs, in %, on a lateral branch that may avoid unintended tripping of the fuse is given by dividing Eq. (6) by $I_{load-max}$, resulting in

$$PL \leq \frac{\sum_{i=1}^{n} I_{i-ibr}}{I_{load-max}} \leq \frac{F_{melt} \cdot I_{fuse}}{SCC \cdot I_{load-max}} \tag{7}$$

The PL is defined in terms of the heavy load current or heavy load demand of the lateral branch, which is common information available to distribution network operators.

B. Conductor Protection

For a fault downstream of the fuse, the maximum current that can flow through the lateral branch conductor must be less than its current conduction limit or admissible thermal current (I_Z). Considering Fig. 1(d), the current flowing through the conductor, right after the fuse, to remain within the conductor conduction limit can be given by

$$F_{melt} \cdot I_{fuse} + SCC \cdot \sum_{i=1}^{n} I_{i-ibr} \leq I_Z \tag{8}$$

where $F_{melt} \cdot I_{fuse}$ represents the maximum current flowing through the fuse at the moment it is about to trip, plus the fault currents of IBRs installed downstream of the fuse until the fault point, given by $SCC \cdot \sum_{i=1}^{n} I_{i-ibr}$.

In Eq. (8), the value of I_Z depends on the conductor type, its material, temperature, and short-circuit duration. To calculate I_Z, Eq. (9) can be used [27]:

$$I_Z = \sqrt{\frac{A \cdot \rho \cdot c \cdot (T_{max} - T_{ini})}{t}} \tag{9}$$

where A is the conductor cross-sectional area (mm^2), ρ is the mass per unit length (kg/m), c is the specific heat capacity (J/kg^{o}C), T_{ini} is the initial temperature of the conductor (^{o}C), T_{max} is the maximum short-circuit temperature of the conductor (^{o}C), and t is the short-circuit duration (s).

Notably, current contributions from IBRs downstream of the fault point are not considered because they do not increase the current in the conductor segment between the fuse and the fault point [25]. Rearranging Eq. (8), to ensure the conductor protection, the rated current of the fuse can be determined by

$$I_{fuse} \leq \frac{I_z - SCC \cdot \sum_{i=1}^{n} I_{i-ibr}}{F_{melt}} \tag{10}$$

To comply with the proposed scheme of Eq. (4), the minimum value of I_{fuse} must be less than or equal to $SCC \cdot \sum_{i=1}^{n} I_{i-ibr}$. Consequently, Eq. (10) can be rewritten by replacing I_{fuse} with $SCC \cdot \sum_{i=1}^{n} I_{i-ibr}$, as presented in Eq. (11a). Rearranging the terms of Eq. (11a), and highlighting the current contribution of the installed IBRs, it gives (11b).

$$SCC \cdot \sum_{i=1}^{n} I_{i-ibr} \leq \frac{I_z - SCC \cdot \sum_{i=1}^{n} I_{i-ibr}}{F_{melt}} \tag{11a}$$

$$\sum_{i=1}^{n} I_{i-ibr} \leq \frac{I_z}{SCC(F_{melt}+1)} \tag{11b}$$

When the condition of (11b) occurs, the boundary condition of Eq. (4) is respected. When it is not, it becomes necessary to evaluate the penetration capacity of the lateral branch or to use other technologies. Depending on the SCC contribution from IBRs and the minimum melting current of the fuse, this limit may vary. Rearranging the terms of Eq. (11b), the ratio between $\sum_{i=1}^{n} I_{i-ibr}$ and I_z is highlighted, is presented in Eq. (12), which can be defined as the penetration capacity (PC) of IBRs for a lateral branch, in %.

$$PC \leq \frac{\sum_{i=1}^{n} I_{i-ibr}}{I_z} \leq \frac{1}{SCC \cdot (F_{melt}+1)} \tag{12}$$

Therefore, it is possible to determine the relationship between the rated current of IBRs that the conductor of a lateral branch can accommodate while guaranteeing conductor protection.

Depending on the value of the SCC and F_{melt}, there will be a maximum value of PC. Table I presents the maximum values of PC for some values of SCC from IBRs for the condition of $F_{melt} = 2$. As the value of SCC increases, the value of PC decreases. The PC has relation of the conductor conduction limit. To calculate PL for this case, it is necessary to relate the currents from all IBRs ($\sum_{i=1}^{n} I_{i-ibr}$) on the lateral branch and the current of the lateral feeder at heady load level ($I_{load-max}$). Dividing Eq. (11b) by $I_{load-max}$ gives (13).

$$PL \leq \frac{\sum_{i=1}^{n} I_{i-ibr}}{I_{load-max}} \leq \frac{\frac{I_z}{SCC(F_{melt}+1)}}{I_{load-max}} \tag{13}$$

which is the penetration level of IBRs, in %, on a lateral branch that may protect the conductor to operate under its current conduction limit.

TABLE I: Penetration capacity of a lateral branch with IBRs in terms of SCC contribution for $F_{melt} = 2$

SCC (p.u.)	Penetration Capacity (%)
1.0	33.3%
1.06	31.4%
1.2	27.8%
1.5	22.2%
2.0	16.7%
3.0	11.1%

C. Sizing the Fuse

The two previous approaches can compute different PL values. Therefore, the lower value of PL between these two is chosen to size the fuse to protect the lateral branch. For the lowest PL, calculate the value of the current flowing backward through the fuse (I_{FS}), of which the maximum is $SCC \cdot \sum_{i=1}^{n} I_{i-ibr}$, and the fault current through the fuse for a fault in the end of the protected lateral, I_{ph-ibr}, to check if there is a value of I_{fuse} that meets Eq. (4). Since changes in conductor cross-section in the lateral branch are uncommon in real-world feeders, they were not considered.

If Eq. (4) is not met, there is the option of keeping the actual fuse of the lateral branch or changing its rated current value to another one, calculating a new value of PL for the approach that generated the lowest PL value previously. The step-by-step of this methodology is summarized in the flow chart shown in Fig. 2.

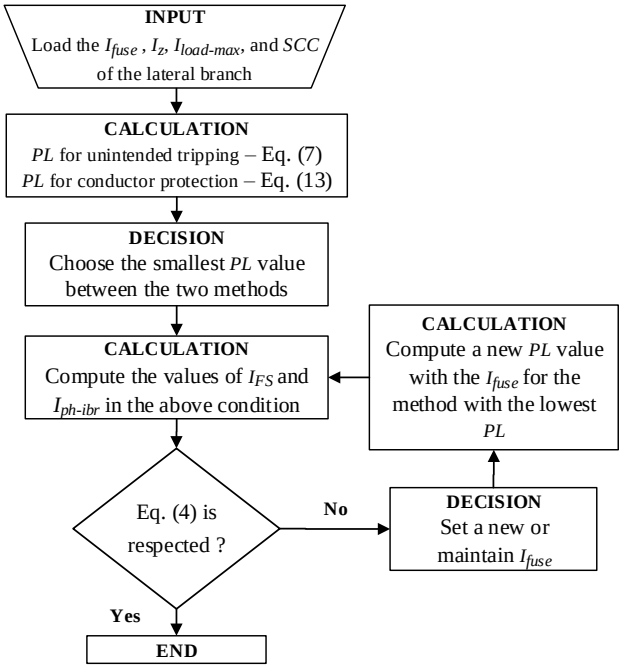

Fig. 2: Flow chart of the methodology to determine the maximum penetration level of IBRs for a lateral branch.

It is important to highlight that the calculated PL values are indicators of attention for distribution network operators

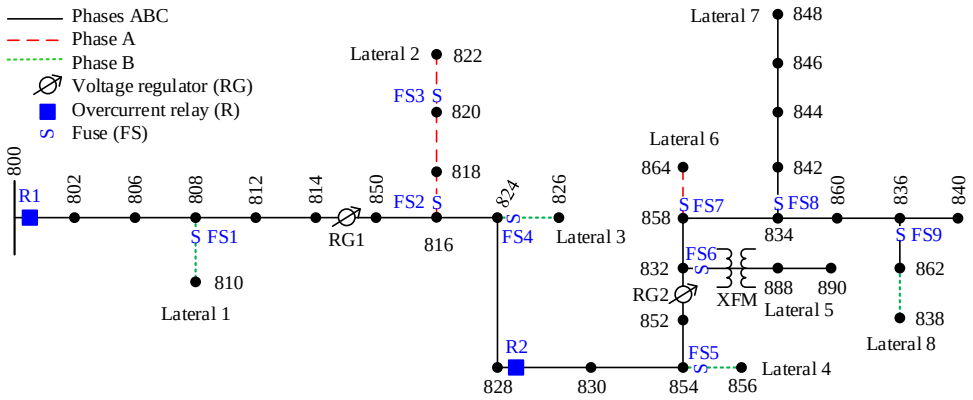

Fig. 3: Single-line diagram of the IEEE 34-node test feeder with overcurrent relays (R) and fuses (FS) placed.

regarding the integration of IBRs. These values should not be considered as an absolute value for limiting the installation capacity of IBRs on the feeder. Additionally, the limitation should not only take into account the protection of the system but also other aspects such as voltage levels, continuous loading of the feeder, among others. Consideration must be given to whether upgrading the protection scheme is more advantageous than limiting IBRs.

IV. Impact on Fuse Protection Scheme

To verify the proposed fuse sizing criteria, the IEEE 34-node test feeder was selected for the case study. This feeder was chosen because it has characteristics that are more similar to real distribution feeders. Firstly, a fuse protection scheme is proposed, without considering the integration of IBRs, as done in [25]. Then, the SCC through the fuses with IBRs was analyzed for a high penetration level. The simulations were run on MATLAB/Simulink. Finally, a fuse sizing approach is proposed considering methods to avoid unintended tripping and to protect the lateral branch conductor.

All lateral branches of the IEEE 34-node test feeder were protected by fuses (FS#), and the location of these fuses is represented in Fig. 3. Due to the length of Lateral 2, it has two fuses. The fuses were sized using Eq. (1). $I_{load-max}$ and I_{ph-min} values were taken from the IEEE report and are presented, for each fuse, in Table II. The type K fuse link was used for all lateral branches.

TABLE II: Values of $I_{load-max}$ e I_{ph-min} to size the fuses

	$I_{load-max}$	I_{ph-min}	I_{fuse}
FS1	1.22 A	397.1 A	6K
FS2	13.02 A	157.30 A	25K
FS3	10.62 A	157.30 A	15K
FS4	3.10 A	229.80 A	6K
FS5	0.31 A	173.10 A	6K
FS6	11.70 A	313.20 A	20K
FS7	0.14 A	161.30 A	6K
FS8	16.30 A	154.00 A	25K
FS9	2.09 A	150.70 A	6K

The IBR model used in this research is the model proposed in [28] and [29], developed in the MATLAB/Simulink environment. This IBR model is a single-phase generator that can be aggregated into a three-phase model, with each phase operating independently. Rated power, SCC contribution and power factor, per phase, can be defined by the user. The power factor for the simulations was set to unity.

Considering a scenario of 100% penetration level of IBRs in each lateral branch, the impact on the fuses was analyzed for different SCC contribution values. For IBRs injecting 1.2 p.u. of SCCs into the grid, the actual fuse scheme and values can remain the same. Analyzing Table III, when IBRs inject 2.0 p.u. of SCCs into the grid, the fuse scheme is disrupted for fuses FS2, FS3, FS4, FS6, and FS8. In this scenario, if a fault occurs upstream of the protected lateral branch, a fault current with a value greater than its nominal value may flow through the fuse, violating Eq. (4).

TABLE III: Currents through the fuses with different SCC from IBRs

	$1.5I_{load-max}$ (A)	$1.2\sum_{i=1}^{n} I_{ibri}$ (A)	$2.0\sum_{i=1}^{n} I_{ibri}$ (A)	Fuse link
FS2	19.53	15.62	26.04	25K
FS3	15.93	12.74	21.24	15K
FS4	4.65	3.72	6.20	6K
FS6	17.55	14.04	23.40	20K
FS8	24.45	19.56	32.60	25K

Therefore, it is necessary to determine a fuse rating to meet this new possible condition for the lateral branches or identify the penetration level at which the fuse can ensure lateral branch protection. This analysis was performed for two different lateral branches of the feeder, considering the approaches addressed in Section III.

V. Determining a Penetration Level Indicator

To estimate the PL of IBRs in a lateral branch for fuse sizing, the allowable PL is estimated to prevent unintended tripping and then to protect the conductor, following the proposed approaches. The results were compared, and the lowest value was chosen. This paper compares two different

SCC contribution scenarios, 1.2 p.u. and 2.0 p.u., since IBRs may have different control strategies depending on the manufacturer.

Simulations were conducted to assess the impacts on fuses FS2 and FS8, from Fig. 3. The two fuses were chosen because their laterals have almost identical active power per phase of the loads installed on them (169 kW for Lateral 2 and 180.67 kW for Lateral 7), and they are protected by the same 25K fuse link. Lateral 2 is single-phase (phase A), while Lateral 7 is three-phase. Lastly, Lateral 2 is longer and closer to the substation than Lateral 7. The results for SCCs were obtained through simulations using MATLAB/Simulink. The factor F_{melt} was considered equal to 2, since the S&C Electric Company "K" Speed Positrol Fuse Links [26] were considered. However, the method can be applied to any F_{melt} value.

A. Unintended Tripping and Conductor Protection Penetration Levels

To prevent the unintended tripping of the fuse, the PL is calculated using Eq. (7). For Lateral 2, the maximum load current is equal to 13.02 A, and for Lateral 7, it is 16.30 A, according to Table II. The values of PL for an SCC contribution of 1.2 p.u. and 2.0 p.u. are shown in Table IV. The value of $\sum_{i=1}^{n} I_{ibri}$ is calculated by multiplying the value of PL by $I_{load-max}$.

TABLE IV: Penetration level of laterals 2 and 7 for 1.2 p.u. and 2.0 p.u. of SCC contributions to avoid unintended tripping

	SCC (p.u.)	I_{fuse} (A)	$I_{load-max}$ (A)	PL	$\sum_{i=1}^{n} I_{ibri}$ (A)
Lateral 2	1.2	25	13.02	320%	41.7
(FS2)	2.0	25	13.02	192%	25.0
Lateral 7	1.2	25	16.30	256%	41.7
(FS8)	2.0	25	16.30	153%	25.0

To protect the conductor, the respective PC values for each SCC contribution are shown in Table I, calculated according to Eq. (12). For an SCC of 1.2 p.u., the PC is 27.8%, and for an SCC of 2.0 p.u., the PC is 16.7%. The PL is calculated using Eq. (13). In Lateral 2, the conductor used for phase and neutral is the ACSR #4 6/1, and for Lateral 7, it is the ACSR #2 6/1. Applying Eq. (9), the value of I_Z for ACSR #4 6/1 is 439.5 A, and for ACSR #2 6/1, it is 695.6 A. For both, a 1-second short-circuit duration was considered, with $T_{ini} = 75\ ^{o}$C, $T_{max} = 200\ ^{o}$C, and $c = 900$ J/kg^{o}C. For ACSR #4 6/1, $A = 21.2$ mm^2 and $\rho = 0.081$ kg/m, and for ACSR #2 6/1, $A = 33.6$ mm^2 and $\rho = 0.128$ kg/m. The results are presented in Table V.

B. Comparison and Analysis of Penetration Levels

Comparing the results of Tables IV and V, the approach to avoid unintended tripping resulted in lower values of PL for both lateral branches. It is necessary to verify whether Eq. (4) is satisfied using the conditions of PL from Table IV. Therefore, the value of I_{ph-ibr} must be measured for each penetration level and each SCC contribution. If the conditions of Eq. (4) are not satisfied, it is necessary to decrease the value of PL or modify the fuse link, following the flowchart of Fig. 2.

TABLE V: Penetration level of laterals 2 and 7 for 1.2 p.u. and 2.0 p.u. of SCC contributions for conductor protection

	SCC (p.u.)	I_z (A)	$I_{load-max}$ (A)	PL	$\sum_{i=1}^{n} I_{ibri}$ (A)
Lateral 2	1.2	439.5	13.02	938%	122.1
FS2	2.0	439.5	13.02	563%	73.3
Lateral 7	1.2	695.6	16.30	1,185%	193.2
FS8	2.0	695.6	16.30	711%	115.9

To address this situation, simulations were carried out using the PL from Table IV in the following scenarios:

- A bolted single-phase fault was applied to node 816 for Lateral 2 and a bolted three-phase fault was applied to node 834 for Lateral 7, to obtain the value of I_{FS}; and
- A bolted fault was applied to the end of the protected section (single-phase at node 822 for Lateral 2 and three-phase at node 848 for Lateral 7), to obtain the value of I_{ph-ibr}.

For Lateral 7, the three-phase fault was applied instead of a single-phase fault to obtain the maximum fault current. The results for each lateral branch are shown in Table VI.

TABLE VI: Currents at the penetration levels of IBRs according to the proposed methods

	SCC (p.u.)	PL	I_{FS} (A)	$\frac{1}{4} I_{ph-ibr}$ (A)	Eq. (4) respected?
Lateral 2	1.2	320%	45.14	34.36	No
FS2	2.0	192%	45.15	34.37	No
Lateral 7	1.2	256%	38.61	49.75	No
FS8	2.0	153%	38.46	49.75	No

Analyzing the results in Table VI, for the penetration levels computed all values of I_{FS} (current in reverse through the fuse) are higher than the rating of the 25K fuse. Therefore, the lateral branches do not support the calculated penetration levels, making it necessary to reduce these values. Maintaining the 25K fuse link and applying the steps from the flowchart of Fig. 2, the new penetration levels are for Lateral 2: 160% and 96% for 1.2 p.u. and 2.0 p.u., respectively, and for Lateral 7: 128% and 77% for 1.2 p.u. and 2.0 p.u., respectively, which are lower than the results presented in Table VI. The values of I_{FS}, I_{ph-ibr}, and verification for Eq. (4) are presented in Table VII.

TABLE VII: Final fuse protection for 25K fuse link with IBRs

	SCC (p.u.)	PL	I_{FS} (A)	$\frac{1}{4} I_{ph-ibr}$ (A)	Eq. (4) respected?
Lateral 2	1.2	160%	22.57	36.70	Yes
FS2	2.0	96%	22.57	36.70	Yes
Lateral 7	1.2	128%	19.30	49.88	Yes
FS8	2.0	77%	19.35	49.88	Yes

Using a 30K fuse link, which is feasible since it coordinates with the 15K fuse link (FS3, see Fig. 3), the penetration levels are for Lateral 2: 192% and 115% for 1.2 p.u. and 2.0 p.u., respectively, and for Lateral 7: 153% and 92% for 1.2 p.u. and 2.0 p.u., respectively, which are higher than those for the 25K fuse link.

C. Protection Coordination

To verify the protection coordination between the devices in Fig. 3, relays R1 and R2 must be configured. The pickup currents, curve types, and Time Multiplier Settings (TMS) for each curve are presented in Table VIII [25]. The minimum coordination time interval (CTI) was set to 300 ms for relay-relay coordination and 120 ms for relay-fuse coordination. The current transformer ratio for R1 is 75/5, and for R2, it is 40/5.

TABLE VIII: Relays settings without IBRs connected

		Phase Protection	**Earth Protection**
R1	Pickup (A)	5.5	1.5
	Curve – IEC 60255	EI	EI
	TMS	7.5%	100%
R2	Pickup (A)	7.5	2.1
	Curve – IEC 60255	EI	EI
	TMS	7.5%	100%

To evaluate the overcurrent protection coordination between R2 and FS8, bolted three-phase and single-phase faults were applied at node 834, and the maximum phase currents through R1, R2, and FS8 were analyzed. The same methodology was applied to assess coordination between R1 and FS2 at node 816. Since Lateral 2 is single-phase, only single-phase faults were considered. For each fault scenario, the penetration levels from Table VII and the 30K fuse were applied.

With the 25K fuse installed, the protection coordination among the devices was preserved. For three-phase and single-phase faults at node 834, the CTI between R2 and FS8 ranged from 133.98 ms to 202.13 ms, while the CTI between R1 and R2 varied from 600 ms to 807 ms. For single-phase faults at node 816, the CTI between R1 and FS2 was 356.72 ms. The fault current contribution from IBRs was not sufficient to disrupt coordination.

On the other hand, when using a 30K fuse link, protection coordination was lost for Lateral 7, as the minimum CTI fell below 120 ms (ranging from -280.7 ms to -107.85 ms). For Lateral 2, the CTI between R1 and FS2 decreased from 356.72 ms to 209.15 ms, still above the 120 ms minimum. Consequently, relay settings must be adjusted. One possible approach is to recalculate new coordination curves for R1 and R2, considering the 30K fuse link in both laterals. Another approach, proposed in [25], is to modify the TMS of the relays based on the IBR penetration level in the feeder.

Maintaining the same IBR penetration level as initially presented in this section, new relay curves were set. The phase pickup currents remained unchanged, as they were based on the feeder's rated current and its unbalance at each relay installation point. However, during calculations, the earth pickup current for relay R2 was adjusted to 2.5 A, as its TMS exceeded 120%. This adjustment resulted in a TMS of 100%. The updated relay settings, considering the 30K fuse link in both laterals, are provided in Table IX. Fig. 4 compares the previous and updated phase protection curves of R1 and R2 with the curves of the 25K and 30K fuses. The new R2 curve lies above the 30K fuse link curve throughout the fault current range, ensuring proper coordination. The current of 205 A represents the maximum current between R2 and the fuse installation points (25K and 30K), while 293 A corresponds to the maximum current between R1 and R2, used for device coordination.

TABLE IX: Relays settings considering 30K fuse on Lateral 7

		Phase Protection	**Earth Protection**
R1	Pickup (A)	5.5	1.5
	TMS	8.5%	113%
R2	Pickup (A)	7.5	2.5
	TMS	11.0%	100%

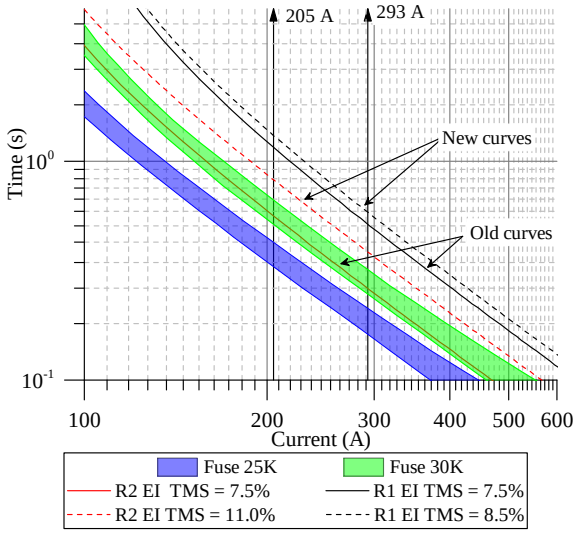

Fig. 4: Phase protection coordination for R1 and R2 considering 25K and 30K fuse links.

D. Discussions

Upgrading the fuse link to a higher value is a decision made by the distribution network operator. It is not mandatory to change the fuse to a higher value; however, this decision allows a higher penetration level for the respective lateral branch. In either case, the distribution network operator is aware of the PL that may start to affect fuse protection.

Clearly, this change alone should not be the sole consideration for feeder overcurrent protection. The fuse rating is used to coordinate with reclosers and relays located upstream, as presented in the previous section. The settings of upstream reclosers and relays can be modified to accommodate the new PL of IBRs. One approach, with or without changing the fuse link, is to modify the TMS of the overcurrent protection curve, maintaining coordination between the OCPDs, as proposed in [25]. The allowance for

greater IBR penetration in the feeder must also align with other technical limits set by the local utility, such as power quality, contingency conditions, and network expansion, for example.

The proposed approach does not require communication links or new infrastructure. Additionally, equipment with the same characteristics as those already in use can be applied.

High penetration levels above 100% or even 200% may seem unusual. However, this can depend on the type of source used to generate electrical energy and the local utility's regulations for distributed generation installation. The Brazilian case illustrates a situation where high penetration levels may occur or is already occurring.

VI. Conclusion

A methodology was proposed in this paper enabling the sizing of the fuses installed in distribution feeders to accommodate a higher penetration of IBRs or to determine the penetration level allowed on it to maintain the current fuse. The method does not require communication links or equipment different from those already in use, and it guarantees the protection of the conductor and prevents the unintended tripping of the fuse. The higher the SCC capacity of the IBR, the lower the penetration level allowed for the protected branch. The high penetration scenarios suggested in the paper may arise due to the non-coincidence between load demands and the generation of IBRs. This factor should be considered when designing the entire feeder protection, since other criteria such as power quality and contingency situations must also be met.

References

[1] D. Lew, M. Asano, J. Boemer, C. Ching, U. Focken, R. Hydzik, M. Lange, and A. Motley, "The Power of Small: The Effects of Distributed Energy Resources on System Reliability," *IEEE Power and Energy Magazine*, vol. 15, no. 6, pp. 50–60, Nov. 2017.

[2] M. C. Vargas, M. A. Mendes, and O. E. Batista, "Fault Current Analysis on Distribution Feeders with High Integration of Small Scale PV Generation," in *2019 IEEE Power & Energy Society General Meeting (PESGM)*, Aug. 2019, pp. 1–5.

[3] M. Meskin, A. Domijan, and I. Grinberg, "Impact of distributed generation on the protection systems of distribution networks: analysis and remedies – review paper," *IET Generation, Transmission & Distribution*, vol. 14, no. 24, pp. 5944–5960, Dec. 2020.

[4] G. Kou, L. Chen, P. Vansant, F. Velez-Cedeno, and Y. Liu, "Fault Characteristics of Distributed Solar Generation," *IEEE Transactions on Power Delivery*, vol. 35, no. 2, pp. 1062–1064, Apr. 2020.

[5] A. C. Enríquez, *Overcurrent Relay Advances for Modern Electricity Networks*. Elsevier, 2023.

[6] R. C. Dugan and D. T. Rizy, "Electric distribution protection problems associated with the interconnection of small, dispersed generation devices," *IEEE Transactions on Power Apparatus and Systems*, vol. PAS-103, no. 6, pp. 1121–1127, 1984.

[7] P. P. Barker and R. W. De Mello, "Determining the impact of distributed generation on power systems. I. Radial distribution systems," in *2000 Power Engineering Society Summer Meeting*, vol. 3, 2000, pp. 1645–1656.

[8] J. K. Tailor and A. H. Osman, "Restoration of fuse-recloser coordination in distribution system with high DG penetration," in *IEEE Power and Energy Society 2008 General Meeting: Conversion and Delivery of Electrical Energy in the 21st Century, PES*, 2008.

[9] S. Chaitusaney and A. Yokoyama, "Prevention of Reliability Degradation from Recloser–Fuse Miscoordination Due To Distributed Generation," *IEEE Transactions on Power Delivery*, vol. 23, no. 4, pp. 2545–2554, Oct. 2008.

[10] H. A. Abdel-Ghany, A. M. Azmy, N. I. Elkalashy, and E. M. Rashad, "Optimizing DG penetration in distribution networks concerning protection schemes and technical impact," *Electric Power Systems Research*, vol. 128, pp. 113–122, Nov. 2015.

[11] A. Elmitwally, E. Gouda, and S. Eladawy, "Restoring recloser-fuse coordination by optimal fault current limiters planning in DG-integrated distribution systems," *International Journal of Electrical Power & Energy Systems*, vol. 77, pp. 9–18, May 2016.

[12] Y. Zhang and R. A. Dougal, "Novel dual-FCL connection for adding distributed generation to a power distribution utility," *IEEE Transactions on Applied Superconductivity*, vol. 21, pp. 2179–2183, Jun. 2011.

[13] H. Yamaguchi and T. Kataoka, "Current limiting characteristics of transformer type superconducting fault current limiter with shunt impedance and inductive load," *IEEE Transactions on Applied Superconductivity*, vol. 18, no. 2, pp. 668–671, Jun. 2008.

[14] H. C. Jo, S. K. Joo, and K. Lee, "Optimal placement of superconducting fault current limiters (SFCLs) for protection of an electric power system with distributed generations (DGs)," *IEEE Transactions on Applied Superconductivity*, vol. 23, no. 3, 2013.

[15] A. Elmitwally, E. Gouda, and S. Eladawy, "Restoring recloser-fuse coordination by optimal fault current limiters planning in DG-integrated distribution systems," *International Journal of Electrical Power & Energy Systems*, vol. 77, pp. 9–18, May 2016.

[16] B. Fani, F. Hajimohammadi, M. Moazzami, and M. J. Morshed, "An adaptive current limiting strategy to prevent fuse-recloser miscoordination in PV-dominated distribution feeders," *Electric Power Systems Research*, vol. 157, pp. 177–186, 2018.

[17] F. Hajimohammadi, B. Fani, and I. Sadeghkhani, "Fuse saving scheme in highly photovoltaic-integrated distribution networks," *International Transactions on Electrical Energy Systems*, vol. 30, no. 1, pp. 1–23, 2020.

[18] M. Dadkhah, B. Fani, E. Heydarian-Forushani, and M. Mohtaj, "An off-line algorithm for fuse-recloser coordination in distribution networks with photovoltaic resources," *International Transactions on Electrical Energy Systems*, vol. 30, no. 9, pp. 1–16, 2020.

[19] A. Barranco-Carlos, C. Orozco-Henao, J. Marin-Quintero, J. Mora-Florez, and A. Herrera-Orozco, "Adaptive Protection for Active Distribution Networks: An Approach Based on Fuses and Relays with Multiple Setting Groups," *IEEE Access*, vol. 11, no. Mar., pp. 31 075–31 091, 2023.

[20] M. Yousaf, A. Jalilian, K. M. Muttaqi, and D. Sutanto, "An Adaptive Overcurrent Protection Scheme for Dual-Setting Directional Recloser and Fuse Coordination in Unbalanced Distribution Networks with Distributed Generation," *IEEE Transactions on Industry Applications*, vol. 58, no. 2, pp. 1831–1842, 2022.

[21] K. Agarwal, J. Benzaquen, and D. Divan, "IFuse - A Controllable Overcurrent Protection Device for Multi-Inverter Microgrids with High IBR Penetration," *Conference Proceedings - IEEE Applied Power Electronics Conference and Exposition - APEC*, pp. 1828–1834, 2023.

[22] T. A. Short, *Electric Power Distribution Handbook*, 2nd ed., C. Press, Ed., Boca Raton, FL, 2014.

[23] Eletrobrás, *Protection of Overhead Distribution Power Systems [Proteção de Sistemas Aéreos de Distribuicao]*, E. Campus, Ed., Rio de Janeiro, Brasil, 1982, vol. 2.

[24] IEEE Std 1547-2018, "IEEE Standard for Interconnection and Interoperability of Distributed Energy Resources with Associated Electric Power Systems Interfaces," p. 138, 2018.

[25] M. C. Vargas, O. E. Batista, and Y. Yang, "Estimation Method of Short-Circuit Current Contribution of Inverter-Based Resources for Symmetrical Faults," *Energies*, vol. 16, no. 7, p. 3130, Mar. 2023.

[26] S&C Electric Company. [Online]. Available: https://www.sandc.com/en/contact-us/time-current-characteristic-curves/

[27] IEC 60949, "Calculation of Thermally Permissible Short-Circuit Currents, Taking into Account Non-Adiabatic Heating Effects," p. 25, 1988.

[28] M. A. Mendes, M. C. Vargas, O. E. Batista, Y. Yang, and F. Blaabjerg, "Simplified Single-phase PV Generator Model for Distribution Feeders with High Penetration of Power Electronics-based Systems," in *2019 IEEE 15th Brazilian Power Electronics Conference and 5th IEEE Southern Power Electronics Conference, COBEP/SPEC 2019*, Dec. 2019, pp. 1–7.

[29] M. C. Vargas, M. A. Mendes, L. G. R. Tonini, and O. E. Batista, "Grid Support of Small-scale PV Generators with Reactive Power Injection in Distribution Systems," in *2019 IEEE PES Innovative Smart Grid Technologies Conference - Latin America (ISGT Latin America)*. Gramado: IEEE, Sep. 2019, pp. 1–6.